Scotia arc kinematics from GPS geodesy

R. Smalley Jr.,[1] I. W. D. Dalziel,[2] M. G. Bevis,[3] E. Kendrick,[3] D. S. Stamps,[1] E. C. King,[4] F. W. Taylor,[2] E. Lauría,[5] A. Zakrajsek,[6] and H. Parra[7]

Received 20 August 2007; revised 1 October 2007; accepted 15 October 2007; published 14 November 2007.

[1] GPS crustal velocity data from the Scotia and South Sandwich plates, transform azimuths, spreading data, and an updated earthquake slip vector catalog provide the first Scotia and South Sandwich plate Euler vector estimates not dependent on closure as the GPS data tie them to the global plate circuit. Neither the GPS data, which sample limited portions of the plates, nor the geologic data, which are not tied to the global spreading circuit, are sufficient individually to define the Euler vectors. As Scotia plate GPS measurements do not sample the stable plate interior, plate boundary deformation field modeling is necessary for Euler vector estimation. Our South America-Antarctic and Scotia-South Sandwich Euler pole estimates agree with previous estimates from either GPS or geologic data. Our South America-Scotia Euler vector, however, is significantly different and near the South America-Antarctic Euler vector producing an approximately coaxial motion of Scotia between South America and Antarctica. **Citation:** Smalley, R., Jr., I. W. D. Dalziel, M. G. Bevis, E. Kendrick, D. S. Stamps, E. C. King, F. W. Taylor, E. Lauría, A. Zakrajsek, and H. Parra (2007), Scotia arc kinematics from GPS geodesy, *Geophys. Res. Lett.*, *34*, L21308, doi:10.1029/2007GL031699.

1. Introduction

[2] Current South America with respect to Antarctic motion is east-west and left-lateral, with plate interaction distributed along the North and South Scotia Ridge transforms (NSRT, SSRT) (Figures 1a and 1b). These transforms are closely associated with the physiographic North and South Scotia ridges, prominent discontinuous bathymetric highs defining the northern and southern limits of the Scotia arc. Within the Scotia arc one finds the Scotia and South Sandwich plates; two small, young, principally oceanic plates. The Scotia plate formed in response to relative movements of the South America and Antarctic plates, while the South Sandwich plate is the result of spreading behind the active South Sandwich arc that closes the eastern end of the entire Scotia arc [*Barker et al.*, 1991; *Barker*, 2001]. The Scotia plate evolved over the past ~30 Myr, incorporating continental fragments torn off South America. Its current identity and relatively simple plate geometry dates back ~6 Myr, when spreading ceased on an extinct northeast-southwest spreading ridge frozen in the Scotia plate. A low, but notable, level of seismicity is associated with this and several other fossil microplate boundaries in the region. *Barker* [2001] suggests the two plate model may be oversimplified as Scotia arc components continue to adjust in a non-rigid manner to the boundary conditions applied by the South America and Antarctic plates. The NSRT and SSRT are long, principally left-lateral strike-slip structures. To the west, the Scotia arc is bounded by the Shackleton fracture zone (SFZ), which is divided into two segments at the intersection of the extinct Antarctic-Phoenix ridge. Northwest of the intersection, focal mechanisms show underthrusting of the Antarctic plate beneath the Scotia plate in the Chile trench (CT), while to the southeast one finds a change to left-lateral strike-slip motion. To the east, the Scotia plate is separated from the South Sandwich plate by the vigorously spreading East Scotia ridge (ESR), a N-S oriented, back-arc ridge across which the South Sandwich plate moves rapidly eastward with respect to the Scotia, South America and Antarctic plates. Westward subduction of South America beneath the South Sandwich plate accommodates Scotia arc areal growth. This subduction has been a constant, essential feature in the complex development of the Scotia arc from its initiation [*Barker*, 2001].

2. Geodetic Sampling of the Scotia Arc

[3] The Scotia and South Sandwich plates have little subaerial exposure for making geodetic measurements and the subaerial parts are not located in their stable plate interiors. The largest Scotia plate subaerial exposure is the portion of Tierra del Fuego on the south side of the left-lateral Magallanes-Fagnano Fault system (MFFS) (Figures 1a and 2a), which is the landward continuation of the NSRT and the current, active plate boundary. The Tierra del Fuego component of the GPS network, therefore, spans the deforming boundary region. The Magallanes-Fagnano Fault system crustal motion field has been modeled as an east-west oriented, left-lateral, strike-slip plate boundary with a 15 km locking depth and a relative velocity of 6.6 ± 1.3 mm/yr [*Smalley et al.*, 2003].

[4] An approximately equilateral triangular-shaped block, the Elephant Island (EI) block, is located where the Shackleton fracture zone, SSRT, South Shetlands trench (SST), and the axis of opening in the Bransfield basin intersect at the northern end of the Antarctic Peninsula (Figures 2a and 2b). This is a region of complex, ongoing adjustment to the extinction of the Antarctic-Phoenix ridge ~4 Ma, which amalgamated the small remaining portion of the Phoenix plate into the Antarctic plate [*Klepeis and Lawver*, 1996; *Larter and Barker*, 1991]. There is ongoing

[1]Center for Earthquake Research and Information, University of Memphis, Memphis, Tennessee, USA.
[2]Institute for Geophysics, John A. and Katherine G. Jackson School of Geoscience, University of Texas at Austin, Texas, USA.
[3]School of Earth Sciences, Ohio State University, Columbus, Ohio, USA.
[4]British Antarctic Survey, Cambridge, UK.
[5]Instituto Geográfico Militar de Argentina, Buenos Aires, Argentina.
[6]Instituto Antártico Argentino, Buenos Aires, Argentina.
[7]Instituto Geográfico Militar de Chile, Santiago, Chile.

0094-8276/07/2007GL031699$05.00

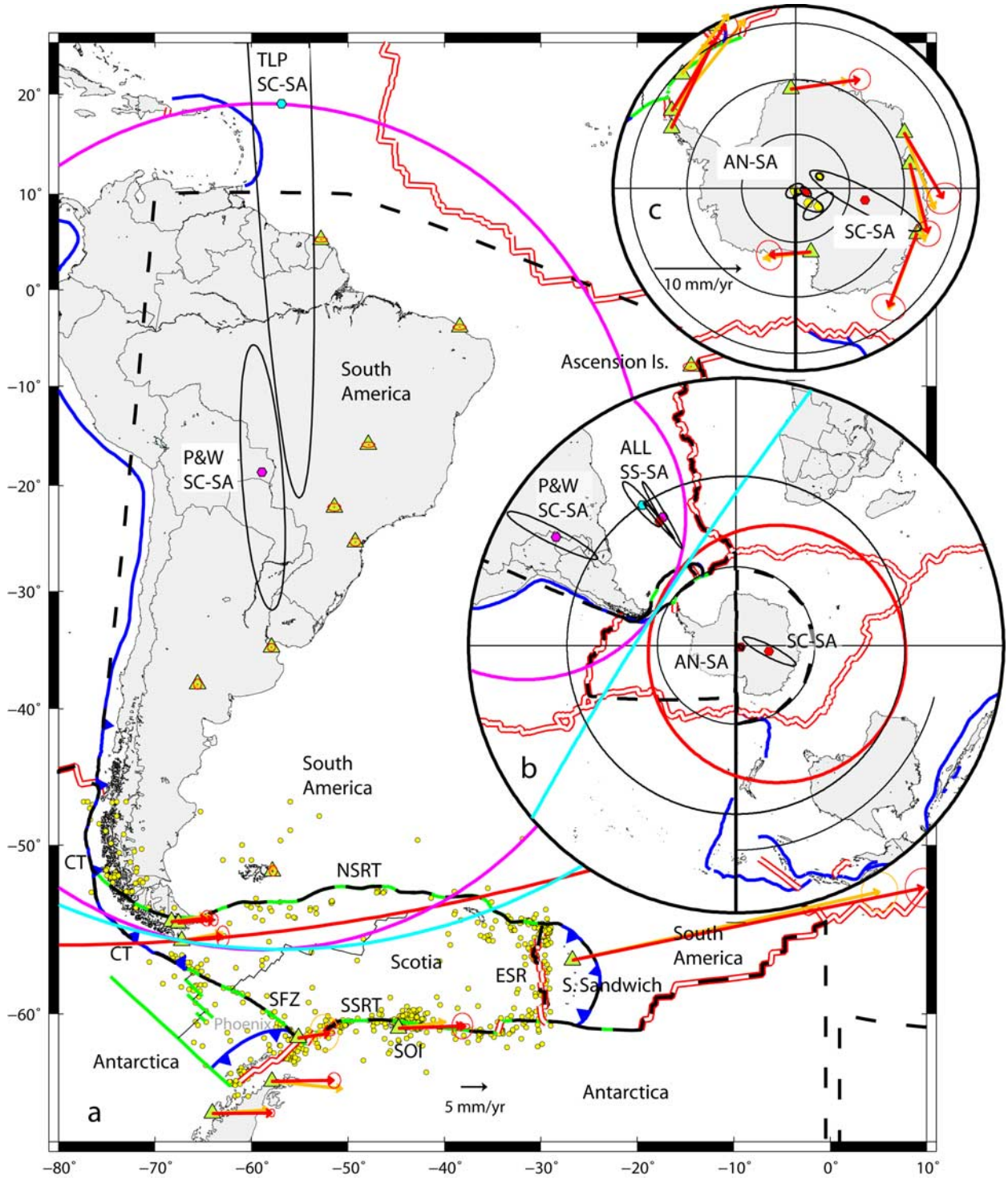

Figure 1. Maps of tectonics, crustal velocities, and Scotia, South Sandwich, and Antarctic with respect to South America Euler poles. Abbreviations defined in text. Plate boundaries (after Plate Project, Institute for Geophysics, University of Texas at Austin): ridges, double red lines; trenches, blue; transforms/fracture zones, green. Thin black lines crossing Scotia and bounding extinct Phoenix plates show extinct ridges. Blocks/plates for DEFNODE, heavy dashed black lines. Blocks are not allowed to cross the prime meridian or date-line so Antarctic plate broken into two blocks that are constrained to have the same Euler vector. Velocities: GPS, orange; model, red; with 95% confidence ellipses. Euler poles shown by hexagons: red, this study; magenta, *Pelayo and Wiens* [1989]; cyan, *Thomas et al.* [2003]. Color coded small circles drawn about South America-Scotia pole passing through Cape Horn GPS station. Seismicity from IRIS DMC catalog, yellow circles. (a) Overview. (b) As in Figure 1a for polar region showing new Scotia-South America pole. (c) GPS velocities defining Antarctic-South America plate motion. Cluster of yellow hexagons near South Pole shows various Antarctic-South America pole estimations: NUVEL-1A [*DeMets et al.*, 1994], REVEL [*Sella et al.*, 2002], *Kreemer et al.* [2003], and *Prawirodirdjo and Bock* [2004].

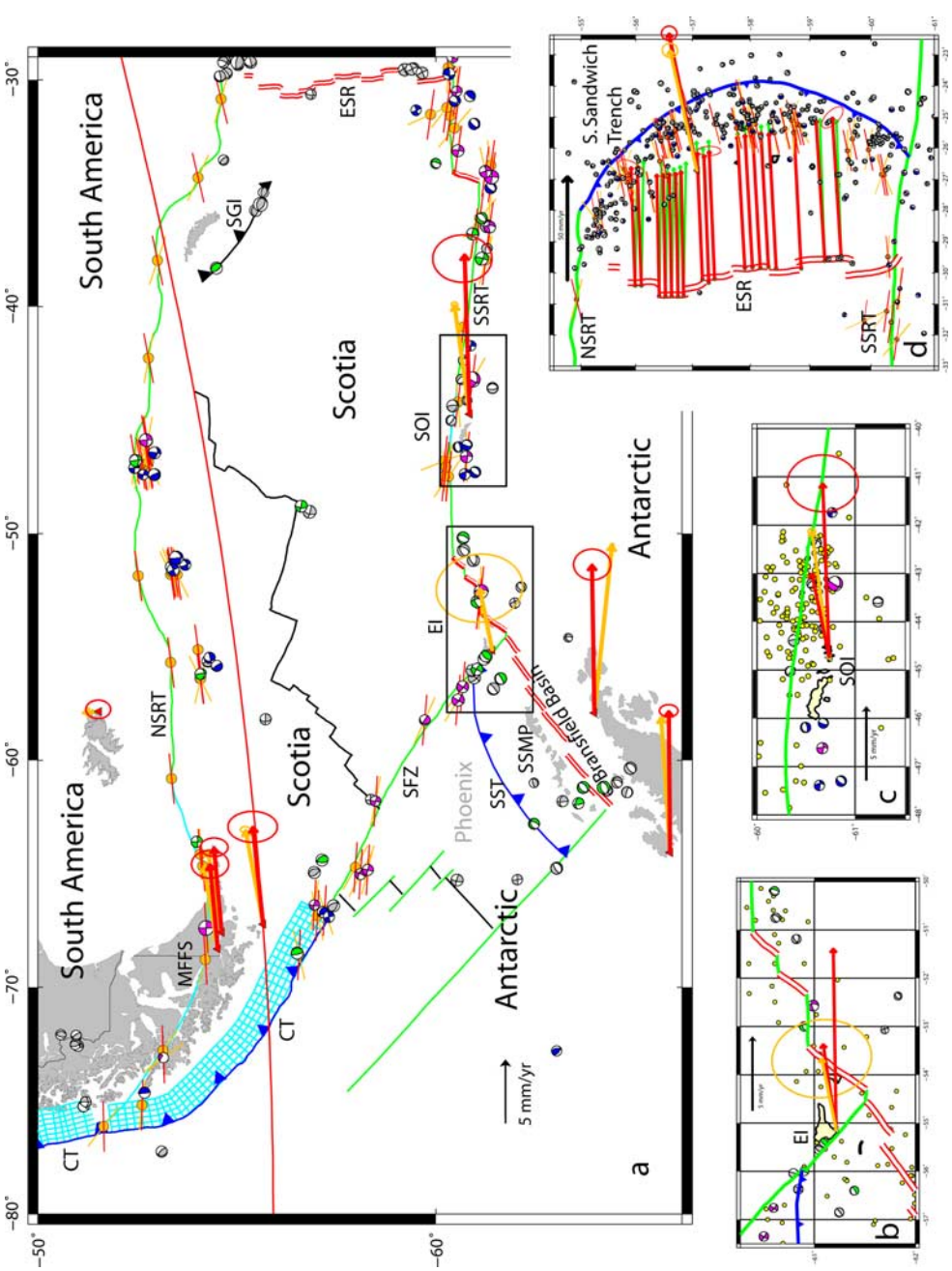

Figure 2. Slip vectors: data, orange; predicted, red. Focal mechanisms: green, *Pelayo and Wiens* [1989]; blue, *Thomas et al.* [2003]; magenta, new; grey, not used. Faults in cyan. East Scotia ridge spreading: green, data; red, predicted. Other features as in Figure 1. (a) Scotia plate. (b) Elephant Island. (c) South Orkney Islands. Short/long model vectors for Scotia/Antarctic plate affinities. (d) South Sandwich plate. Error ellipses shown on 3 vectors, orientation on others varies smoothly.

debate whether subduction along the South Shetlands trench slowed down or ceased with extinction of the ridge [*Larter and Barker*, 1991; *Robertson Maurice et al.*, 2003; *Fretzdorff et al.*, 2004]. Opening across the Bransfield basin is not organized into normal seafloor spreading [*Lawver et al.*, 1996], but has been confirmed and quantified by GPS measurements [*Dietrich et al.*, 2001; F. W. Taylor et al., manuscript in preparation, 2007]. *Barker et al.* [1991] proposed a new microplate, the South Shetlands microplate (SSMP), with boundaries along the South Shetlands trench and the Bransfield Basin. The westernmost section of the SSRT is a complex zone of alternating transform segments and releasing bend step-overs along-strike of the Bransfield Basin. Focal mechanisms in the step-overs indicate normal faulting compatible with the strike-slip segments. *Klepeis and Lawver* [1996] suggest, based on earthquake [*Pelayo and Wiens*, 1989] and marine geophysical data, that the Elephant Island block is being transferred to the Antarctic plate across an east-west striking fault developing along its northern side.

[5] The only other significant Scotia arc subaerial exposure is South Georgia Island (SGI) (Figure 2a), a continental fragment detached from the southeastern tip of South America during formation of the Scotia arc [*Dalziel et al.*, 1974]. The island is located in a NSRT restraining bend and is most likely a microplate or block with the main strike-slip plate boundary to the northeast and a thrust system, along which it is uplifted, to the southwest. Assignment of South Georgia Island to a specific plate is not strongly constrained. Following *Forsyth* [1975], *Pelayo and Wiens* [1989] draw the plate boundary through South Georgia Island and their Scotia-South America Euler pole depends strongly on an event southwest of the island that represents underthrusting of Scotia beneath South America (Figure 2a). *Thomas et al.* [2003] have better sampling of NSRT events and place the island on the Scotia plate, which rules out using the thrust event in their inversion. South Georgia Island had to have been on the Scotia side of the boundary to have been displaced to its current location and we associate it with the Scotia plate.

[6] The South Sandwich plate has the two most active plate boundaries in the Scotia arc, the rapidly spreading East Scotia ridge and the South Sandwich trench. In the South Sandwich trench the rapid rates of both subduction and back arc spreading and the lack of large, shallow underthrusting earthquakes indicate this plate boundary is seismically decoupled or unlocked [*Scholz and Campos*, 1995; *Bevis et al.*, 1995]. The outer trench rise, where the South America plate is rapidly rolling back, is also unusually seismically active having numerous normal faulting events (Figure 2d). The only subaerial South Sandwich plate exposures are the active, potentially deforming volcanic islands of the South Sandwich arc.

3. Data, Analysis, and Discussion

[7] Having only transform or subduction boundaries with their other neighbors, neither the Scotia nor South Sandwich plates have the rate data necessary to tie into the global spreading circuit and could therefore not be included in the NUVEL1 plate model [*DeMets et al.*, 1990]. The Scotia and South Sandwich plates are separated by a spreading boundary (Figures 1a and 2d) so their relative motion can be determined from magnetic anomaly data. Previous estimates for Scotia and South Sandwich Euler poles relative to South America and Antarctica (Figure 1a) were based on earthquake slip vectors, transform fault azimuths and plate circuit closure [*Pelayo and Wiens*, 1989; *Thomas et al.*, 2003]. The Scotia and South Sandwich plates were subsequently included in NUVEL-1A, also using closure [*DeMets et al.*, 1994]. Recent GPS measurements from the Scotia [*Smalley et al.*, 2003] and South Sandwich [*King et al.*, 1997] plates provide the rate constraints needed to determine global plate motion Euler vectors for both plates not dependent on closure.

[8] *Pelayo and Wiens* [1989] and *Thomas et al.* [2003] discuss in detail their selections of geologic observations and slip vectors based on bathymetric, magnetic and earthquake data. Small scale complexity produces significant complications, especially along the SSRT where there are a number of amalgamated microplates and high angle releasing bend offsets. Low seismicity rates along the NSRT and SSRT also suggest slow rates of motion between the South America-Scotia and Antarctic-Scotia plate pairs. Except for a few changes discussed below, this study combines new GPS and earthquake slip data with the data presented by *Thomas et al.* [2003]. The slip vector data from the Global (formerly Harvard) CMT catalog [*Dziewonski et al.*, 1981] was updated, with ~20 new events plus a focal mechanism (P. Alvarado, personal communication, 2007) for a 1949, M = 7.4, Magallanes-Fagnano Fault event in Tierra del Fuego. Simply combining the GPS data with the input data set of *Thomas et al.* [2003] resulted in a value of reduced χ^2 of 2.3. Increasing the earthquake slip vector uncertainty from 15° to 20°, while leaving the uncertainty values for other types of data from *Thomas et al.* [2003] unchanged resulted in a reduced χ^2 of less than 2. *Thomas et al.* [2003] used 1° averages of the trends of seafloor lineaments from sidescan images to estimate East Scotia ridge transform azimuth data but do not report spreading directions. In our inversion, we read the azimuths for the spreading data from the rose diagrams by *Thomas et al.* [2003] and applied them over 1° segments. We did not use the four East Scotia ridge transform azimuths of *Thomas et al.* [2003].

[9] The combined GPS-geologic data set (available in the auxiliary material)[1] was inverted for motions of the Scotia, South Sandwich, and Antarctic plates with respect to the South America plate using the program DEFNODE (R. McCaffrey, DEFNODE users guide, available at http://www.rpi.edu/~mccafr/defnode/, 1995), which inverts for Euler vectors using slip vector, transform azimuth, spreading (rate and direction), and GPS data. The GPS data can sample both stable plate interiors (blocks) and deforming plate boundary regions. By defining plate boundary fault geometries, DEFNODE uses backslip [*Savage*, 1983] and elasticity [*Okada*, 1985, 1992] to model the associated deformation which is added to the plate movement in the inversion. We included modeling deformation associated with the left-lateral strike-slip Magallanes-Fagnano Fault system of the Scotia-South America boundary and the subduction of Antarctica beneath both the South America and Scotia plates along the Chile trench, all of which affect GPS sites in southern Tierra del Fuego (Figure 2a). Modeling left-lateral strike-slip deformation associated with

[1] Auxiliary materials are available in the HTML. doi:10.1029/2007GL031699.

Table 1. Geographic Coordinates[a]

Fixed	Moving	Long.	Lat.	Omega	σ Omega	Emax	Emin	Azi
SAMR	SCOT	99.8056	−76.9866	−0.0817	0.0113	11.40	2.17	252.55
SAMR	SAND	328.2674	−37.2098	1.7634	0.4379	7.47	0.58	98.09
SAMR	ANT	109.1671	−88.0066	−0.2206	0.0046	1.22	0.66	246.09
SCOT	SAND	328.8343	−39.4586	1.8033	0.4443	6.53	0.61	98.03
SCOT	ANT	273.2310	−85.5743	−0.1413	0.0147	5.06	1.62	236.00
SAND	ANT	328.4657	−42.6208	−1.9005	0.4512	5.17	0.54	280.50

[a]Euler vectors for plate motions with respect to fixed South America plate for preferred solution. Positive rate is counter-clockwise rotation with respect to fixed plate. Rates in degrees/My. SAMR, South America; SCOT, Scotia; SAND, South Sandwich; ANT, Antarctic plates.

the Scotia-Antarctic plate boundary on the SSRT, which affects the GPS site on the South Orkney Islands (SOI) (Figures 2a and 2c), was also included.

[10] The SSRT is relatively well sampled by earthquakes, but NSRT seismicity is highly clustered and long segments are quiet seismically. Additionally, in the restraining bend near South Georgia Island, slip vectors may not show plate motion due to slip partitioning [*McCaffrey*, 1992, 1993]. Although the NSRT only came into its current existence when the Scotia plate formed and inherited its morphology from previous plate interactions, it now represents a principally transform boundary that can provide important geometrical constraints in regions without seismicity. We performed the inversion with and without transform azimuths distributed approximately uniformly along the NSRT. The poles for the two cases differ latitudinally by ~10°. The result obtained without the NSRT transform data has a slightly smaller reduced χ^2 (1.612 vs. 1.736), but, we prefer the estimate with the transform data included as it significantly increases sampling of the NSRT plate boundary geometry and decreases the parameter uncertainties (Figure 2a) (preferred result in Tables 1 and 2, other in auxiliary material).

[11] Our preferred Euler vector for Scotia-South America is approximately parallel to that for Antarctic-South America motion (Figure 1b); indicating overall motions of Scotia and Antarctica with respect to South America differ primarily in speed, not direction. The new Scotia-South America Euler pole differs significantly from those of *Pelayo and Wiens* [1989] and *Thomas et al.* [2003]. All three poles, however, lie roughly on a ~N-S oriented great circle perpendicular to the Scotia plate's long east-west axis. The error ellipses are noticeably elongated parallel to this great circle. This illustrates the classic trade-off between Euler pole position and rate when data are restricted to a small range of Euler latitudes and longitudes. The small circle about the new South America-Scotia Euler pole matches the overall shape of the NSRT better than small circles about the two previous estimates. The recumbent "S" shape of the NSRT is incompatible with a small circle, and local transtensional and transpressional regions there result from the boundary not following a small circle. These local effects are superimposed on an overall transpressional NSRT and transtensional SSRT. The SSRT lies approximately on the 61°S parallel, which is also in good agreement with the Scotia-Antarctic pole being near the South Pole.

[12] Predicted motion along the Shackleton fracture zone between the Antarctic and Scotia plates is transpressive with an approximately constant angle and highly oblique subduction would be expected along the whole boundary. This is in contrast to the sharp change in gravity anomaly and focal mechanism character along the Shackleton fracture zone at the intersection of the extinct Antarctic-Phoenix ridge (Figure 2a). Focal mechanisms indicate subduction in the Chile trench northwest of the intersection and strike-slip motion to the southeast where slip vectors correlate better with the morphology [*Livermore et al.*, 2004] and plate motion before amalgamation of the Phoenix plate, than with current plate motions. We postulate a convergent plate boundary, whose polarity is not obvious, consistent with current plate motions is developing along this segment of the Shackleton fracture zone.

[13] The GPS site on Elephant Island, surprisingly, is moving as if it is part of the stable Scotia plate (Figure 2b), not only for our new results but also those of *Pelayo and Wiens* [1989] and *Thomas et al.* [2003]. This contrasts with more geologically based models, such as that of *Klepeis and Lawver* [1996] mentioned previously. Predicted motions for Antarctic plate affinity show Elephant Island is clearly not moving with the Antarctic plate. The GPS site on Elephant Island is close to the plate boundary and the general plate geometry around the Elephant Island block suggests it should not be in a stable area of the Scotia plate. The large GPS error ellipse allows movement with respect to the Scotia plate but it cannot be currently quantified. Elephant Island also seems to be moving distinctly with respect to the South Shetlands microplate (F. W. Taylor et al., manuscript in preparation, 2007). Unfortunately, the GPS data currently cannot address geologically implied vertical movement or deformation of the Elephant Island block. The GPS, seismic, and geologic data from Elephant Island sample different time scales and may be observing the adjustment of the Elephant Island block to recent tectonic changes over different time scales.

Table 2. Cartesian Coordinates[a]

Fixed	Moving	Wx	Wy	Wz	σx	σy	σz	σxy	σxz	σyz
SAMR	SCOT	0.0031	−0.0181	0.0796	0.0052	0.0078	0.0134	0.0000	−0.0001	0.0031
SAMR	SAND	1.1945	−0.7387	−1.0664	0.2258	0.1133	0.3933	−0.0254	−0.0887	1.1945
SAMR	ANT	0.0025	−0.0072	0.2205	0.0026	0.0026	0.0046	0.0000	0.0000	0.0025
SCOT	SAND	1.1913	−0.7205	−1.1460	0.2259	0.1136	0.3935	−0.0254	−0.0888	1.1913
SCOT	ANT	−0.0006	0.0109	0.1409	0.0058	0.0082	0.0141	0.0000	−0.0001	−0.0006
SAND	ANT	−1.1920	0.7314	1.2869	0.2258	0.1133	0.3933	−0.0254	−0.0887	−1.1920

[a]Euler vectors for plate motions with respect to fixed South America plate for preferred solution. Positive rate is counter-clockwise rotation with respect to fixed plate. Rates in degrees/My. SAMR, South America; SCOT, Scotia; SAND, South Sandwich; ANT, Antarctic plates.

[14] Scotia-Antarctic motion along the SSRT is principally left-lateral strike-slip. A continuous GPS station on the South Orkney Islands block, on the south side of the SSRT, is clearly in a deforming plate boundary region. Poor constraints on properties of the plate boundary, one side is oceanic while the other is continental, severely limit modeling deformation related to the plate boundary interaction. The interseismic GPS vector is midway between that predicted for the Scotia and Antarctic plates (Figure 2c). Principally east directed co-seismic displacement associated with a M = 7.6 earthquake on the SSRT, ~75 km east, confirms accumulation of slip deficit occurs there consistent with a left-lateral transform plate boundary.

[15] Results from our inversion for the Scotia-South Sandwich Euler vector, which includes new GPS data from Candlemas Island, are in good agreement with previous determinations [*Pelayo and Wiens*, 1989; *Thomas et al.*, 2003]. The GPS data tie the South Sandwich Euler vector directly to the global plate circuit.

4. Conclusions

[16] New GPS data from the Scotia and South Sandwich plates combined with earthquake slip vector, transform azimuth, and spreading rate data provide the first estimations for their Euler vectors tied directly to the global plate circuit. The new Scotia-South America Euler vector produces approximately coaxial motion of both the South America and Scotia plates about the Antarctic plate. Elephant Island is found to be most closely associated with the Scotia plate and the South Orkney Islands are located in a deforming region on the edge of the Antarctic plate.

[17] **Acknowledgments.** The manuscript was greatly improved due to careful reviews by R. McCaffrey and an anonymous reviewer. We thank the Instituto Geográfico Militar de Argentina, Instituto Geográfico Militar de Chile, Instituto Antártico Argentino, Administración de Parques Nacionales de Argentina, Armada Argentina, Centro Austral de Investigaciones Científicas, Univ. Nac. de La Plata, and Alfred Wegener Institute for collaboration supporting continuous and campaign GPS measurements. Figures made with GMT [*Wessel and Smith*, 1998]. This work was supported by NSF grants OPP-9527529 and EAR-9417514 (Memphis), OPP-9530383 and EAR-9115576 (Ohio), OPP-9526687 (Texas). Contribution numbers: CERI 516, UTIG 8192.

References

Barker, P. F. (2001), Scotia Sea regional tectonic evolution: Implications for mantle flow and palaeocirculation, *Earth Sci. Rev.*, *55*, 1–39.

Barker, P. F., I. W. D. Dalziel, and B. C. Storey (1991), Tectonic development of the Scotia Arc region, in *The Geology of Antarctica*, *Monogr. Geol. Geophys.*, vol. 17, edited by R. J. Tingey, pp. 215–248, Oxford Univ. Press, New York.

Bevis, M., F. W. Taylor, B. E. Chutz, J. Recy, B. L. Isacks, S. Helu, R. Singh, E. Kendrick, J. Stowell, B. Taylor, and S. Calmant (1995), Geodetic observations of very rapid convergence and back-arc extension at the Tonga arc, *Nature*, *374*, 249–251.

Dalziel, I. W. D., M. F. De Wit, and K. F. Palmer (1974), Fossil marginal basin in the southern Andes, *Nature*, *250*, 291–294.

DeMets, C., R. G. Gordon, D. F. Argus, and S. Stein (1990), Current plate motions, *Geophys. J. Int.*, *101*, 425–478.

DeMets, C., R. G. Gordon, D. F. Argus, and S. Stein (1994), Effect of recent revisions to the geomagnetic reversal time scale on estimates of current plate motions, *Geophys. Res. Lett.*, *21*, 2191–2194.

Dietrich, R., et al. (2001), ITRF coordinates and plate velocities from repeated GPS campaigns in Antarctica–An analysis based on different individual solutions, *J. Geod.*, *74*, 756–766.

Dziewonski, A. M., T.-A. Chou, and J. H. Woodhouse (1981), Determination of earthquake source parameters from waveform data for studies of global and regional seismicity, *J. Geophys. Res.*, *86*, 2825–2852.

Forsyth, D. W. (1975), Fault plane solutions and tectonics of the South Atlantic and Scotia Sea, *J. Geophys. Res.*, *80*, 1429–1443.

Fretzdorff, S., T. J. Worthington, K. M. Haase, R. Hékinian, L. Franz, R. A. Keller, and P. Stoffers (2004), Magmatism in the Bransfield Basin: Rifting of the South Shetland Arc?, *J. Geophys. Res.*, *109*, B12208, doi:10.1029/2004JB003046.

King, E. C., M. G. Bevis, R. D. Larter, A. M. Reading, I. W. Dalziel, F. W. Taylor, and R. Smalley (1997), GPS measurements in the South Sandwich arc, *Eos Trans. AGU*, *78*(46), Fall Meet. Suppl., F168.

Klepeis, K. A., and L. A. Lawver (1996), Tectonics of the Antarctic-Scotia plate boundary near Elephant and Clarence Islands, West Antarctica, *J. Geophys. Res.*, *101*, 20,211–20,231.

Kreemer, C., W. E. Holt, and J. A. Haines (2003), An integrated global model of present-day plate motions and plate boundary deformations, *Geophys. J. Int.*, *154*, 8–34.

Larter, R. D., and P. F. Barker (1991), Effects of ridge crest-trench interaction on Antarctic-Phoenix spreading: Forces on a young subducting plate, *J. Geophys. Res.*, *96*, 19,583–19,607.

Lawver, L. A., B. J. Sloan, D. H. N. Barker, M. Ghidella, R. P. von Herzen, R. A. Keller, G. P. Klinkhammer, and C. S. Chin (1996), Distributed, active extensions in Bransfield Basin, Antarctic Peninsula: Evidence from multibeam bathymetry, *GSA Today*, *6*, 1–6.

Livermore, R., G. Eagles, P. Morris, and A. Maldonado (2004), Shackleton fracture zone: No barrier to early circumpolar ocean circulation, *Geology*, *32*, 797–800.

McCaffrey, R. (1992), Oblique plate convergence, slip vectors and forearc deformation, *J. Geophys. Res.*, *97*, 8905–8915.

McCaffrey, R. (1993), On the role of the upper plate in great subduction zone earthquakes, *J. Geophys. Res.*, *98*, 11,953–11,966.

Okada, Y. (1985), Surface deformation to shear and tensile faults in a half-space, *Bull. Seismol. Soc. Am.*, *75*, 1135–1154.

Okada, Y. (1992), Internal deformation due to shear and tensile faults in a half-space, *Bull. Seismol. Soc. Am.*, *82*, 1018–1040.

Pelayo, A. M., and D. A. Wiens (1989), Seismotectonics and relative plate motions in the Scotia region, *J. Geophys. Res.*, *94*, 7293–7320.

Prawirodirdjo, L., and Y. Bock (2004), Instantaneous global plate motion model from 12 years of continuous GPS observations, *J. Geophys. Res.*, *109*, B08405, doi:10.1029/2003JB002944.

Robertson Maurice, S. D., D. A. Wiens, P. J. Shore, E. Vera, and L. M. Dorman (2003), Seismicity and tectonics of the South Shetland Islands and Bransfield Strait from a regional broadband seismograph deployment, *J. Geophys. Res.*, *108*(B10), 2461, doi:10.1029/2003JB002416.

Savage, J. C. (1983), A dislocation model of strain accumulation and release at a subduction zone, *J. Geophys. Res.*, *88*, 4984–4996.

Scholz, C. H., and J. Campos (1995), On the mechanism of seismic decoupling and back arc spreading at subduction zones, *J. Geophys. Res.*, *100*, 22,103–22,115.

Sella, G. F., T. H. Dixon, and A. Mao (2002), REVEL: A model for Recent plate velocities from space geodesy, *J. Geophys. Res.*, *107*(B4), 2081, doi:10.1029/2000JB000033.

Smalley, R., Jr., E. Kendrick, M. G. Bevis, I. W. D. Dalziel, F. Taylor, E. Lauría, R. Barriga, G. Casassa, E. Olivero, and E. Piana (2003), Geodetic determination of relative plate motion and crustal deformation across the Scotia-South America plate boundary in eastern Tierra del Fuego, *Geochem. Geophys. Geosyst.*, *4*(9), 1070, doi:10.1029/2002GC000446.

Thomas, C., R. Livermore, and F. Pollitz (2003), Motion of the Scotia sea plates, *Geophys. J. Int.*, *155*, 789–804.

Wessel, P., and W. H. F. Smith (1998), New, improved version of Generic Mapping Tools released, *Eos Trans. AGU*, *79*(47), 579.

M. G. Bevis and E. Kendrick, School of Earth Sciences, Ohio State University, 275 Mendenhall Laboratory, 125 South Oval Mall, Columbus, OH 43210, USA. (mbevis@osu.edu; kendrick.42@osu.edu)

I. W. D. Dalziel and F. W. Taylor, Institute for Geophysics, John A. and Katherine G. Jackson School of Geoscience, University of Texas at Austin, J. J. Pickle Research Campus, Building 196, 10100 Burnet Road, Austin, TX 78785-4445, USA. (ian@utig.ig.utexas.edu; fred@utig.ig.utexas.edu)

E. C. King, British Antarctic Survey, High Cross, Madingley Road, Cambridge CB3 0ET, UK. (ecki@bas.ac.uk)

E. Lauría, Instituto Geográfico Militar de Argentina, Avenida Cabildo 381 (1426), Ciudad Autónoma de Buenos Aires, Argentina. (elauria@igm.gov.ar)

H. Parra, Instituto Geográfico Militar de Chile, Nueva Santa Isabel 1640, Santiago, Chile. (hparra@igm.cl)

R. Smalley Jr. and D. S. Stamps, Center for Earthquake Research and Information, University of Memphis, 3876 Central Avenue, Suite 1, Memphis, TN 38152, USA. (rsmalley@memphis.edu; dsstamps@memphis.edu)

A. Zakrajsek, Instituto Antártico Argentino, Cerrito 1248 (C1010AAZ), Ciudad Autónoma de Buenos Aires, Argentina. (afz@dna.gov.ar)